Medicinal chemistry

Xiao et al., Med Chem (Los Angeles) 2018, 8:4
DOI: 10.4172/2161-0444.1000496

Research Article Open Access

The Potential Inhibitors in Traditional Chinese Medicine for BCR-ABL T315I Mutation of Chronic Myelogenous Leukemia

Yali Xiao, Pei-Chun Chang* and Jeffrey JP Tsai

Department of Bioinformatics and Medical Engineering, Asia University, Taichung, Taiwan

Abstract

Chronic Myelogenous Leukemia (CML) is a myeloproliferative disorder characterized by the appearance of abnormal proliferation of white blood cells in the Philadelphia chromosome. Current drugs target ABL kinase may have resistance or have risks of serious side effects. We performed molecular docking and 2D-QSAR modeling regarding ABL and its mutant T315I to discover the potential candidate compounds for CML treatment. We present four potent TCM compounds, salvianolic acid C, baicalin, 1,4-dicaffeoylquinic acid, and dihydroisotanshinone I as potential candidates as lead drugs from the TCM compounds. It might have the potential to treat Chronic Myelogenous Leukemia with fewer side effects.

Keywords: Chronic Myelogenous Leukemia; ABL kinase; Molecular docking; 2D-QSAR

Introduction

Chronic Myelogenous Leukemia (CML) is a myeloproliferative disorder characterized by the appearance of abnormal proliferation of white blood cells in the Philadelphia chromosome [1]. Approximately 95% of CML patients have the Philadelphia chromosome [2]. The Philadelphia chromosome is the ABL kinase gene on chromosome 9 fuses with the BCR gene on chromosome 22, the translocation t (9:22) (q34; q11) format Bcr-Abl fusion gene and loss of normal regulatory function. The results are excessive expression of tyrosine kinase, continued activation of the downstream conduction pathway, cell continuous proliferation, and inhibition of apoptosis. Currently, first generation drug for the treatment of CML is Imatinib, the second generation of drugs are Dasatinib, Nilotinib, Bosutinib, the third generation of the drug is Ponatinib [3-5]. Imatinib is a Tyrosine Kinase Inhibitor (TKI) in the clinical treatment of CML that inhibits Bcr-Abl tyrosine kinase activity and cell proliferation, finally induced apoptosis [6]. Sometimes, Imatinib is resistant to patients with Bcr-Abl point mutations. In this condition, patients are evaluated to be treated with second-generation CML tyrosine kinase inhibitors such as Dasatinib, Nilotinib, and Bosutinib. The second generation drugs can inhibit many different types of Bcr-Abl point mutations [4], but there are some cases of drug resistance occurring for point mutation of T315I. In 2012, the United States Food and Drug Administration (FDA) approved Ponatinib as a third-generation CML tyrosine kinase inhibitor that effectively inhibits the T315I point mutation whereas Ponatinib is expensive. In 2013, the FDA requested the manufacturers of Ponatinib to suspend promotion and sales for the sakes of the risk of life-threatening blood clots and severe narrowing of blood vessels.

Currently approved drugs for CML treatment almost exist with discomfort side effects. In addition, Imatinib has drug resistance for Bcr-Abl point mutations. Nilotinib, Dasatinib, and Bosutinib can inhibit Bcr-Abl for different types of point mutations, but could not overcome the consistency of Bcr-Abl T315I mutation. Ponatinib can overcome the T315I mutation of Bcr-Abl to inhibit the function of tyrosine kinase. However, Ponatinib has a serious life-threatening cardiovascular obstruction in humans. In this paper, we combine the Traditional Chinese Medicine (TCM) database with the Chinese herb formula for CML treatments to screen the candidate compounds with similar cytotoxicity to currently approved drugs but less the side effects. We performed molecular docking and 2D-QSAR modeling regarding ABL target and ABL T315I mutant to discover the potential candidate compounds for CML treatment.

Materials and Methods

Molecular docking

The structure of active site of human Bcr-Abl tyrosine kinase and its mutant were downloaded from Protein Data Bank (PDB ID: 2G1T, 2V7A) [7,8]. We collected herb prescription for CML treatment from the Shanghai Chinese herbal prescriptions Innovation Center (http://www.sirc-tcm.sh.cn/en/index.html) [9]. The chemical components of these Chinese herbal medicine prescriptions are combined with the chemical structure from TCM Database@Taiwan [10] to produce the TCM compound library. Molecular docking was performed using the DS2.5 LigandFit module with the force field of HARVard Macromolecular Mechanics (CHARMm) to screen out the candidate compounds. The candidate compounds were assessed based on DockScore and ADMET pharmacokinetic properties, including absorption, solubility, BBB, and PPB.

2D-Quantitative Structure-Activity Relationship models (2D-QSAR)

In this study, 18 candidate inhibitors were collected (Table 1) from the literature [5] with biological activity pIC50 regarding Bcr-Abl and Bcr-Abl T315I. We randomly assigned to training group and test group containing 14 compounds and 4 compounds, respectively. The chemical structures of these inhibitors were drawn with ChemDraw Ultra 10.0 (CambridgeSoft Inc., USA) and transform into the 3D structure using Chem3D Ultra 10.0 (CambridgeSoft Inc., USA). We applied the DS 2.5 Calculate Molecular Property Module to calculate the molecular descriptors for each inhibitor. Based on these molecular descriptors and corresponding pIC50 value, the genetic function approximation model (GFA) was used to select the high correlation (R^2>0.8) molecular characteristics to build the 2D-QSAR model of biological activity (pIC 50). We used the training set compounds to build multiple linear

***Corresponding author:** Pei-Chun Chang, Department of Bioinformatics and Medical Engineering, Asia University, Taichung, Taiwan, Tel: 886423323456; E-mail: peichun.chang@gmail.com

Received April 02, 2018; **Accepted** April 06, 2018; **Published** April 10, 2018

Citation: Xiao Y, Chang PC, Tsai JJP (2018) The Potential Inhibitors in Traditional Chinese Medicine for BCR-ABL T315I Mutation of Chronic Myelogenous Leukemia. Med Chem (Los Angeles) 8: 066-078. doi: 10.4172/2161-0444.1000496

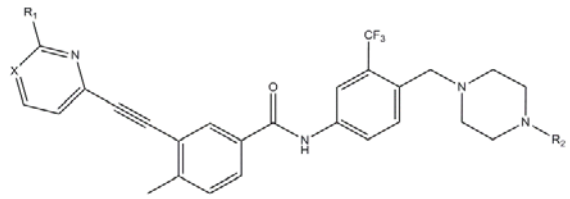

7a -7f

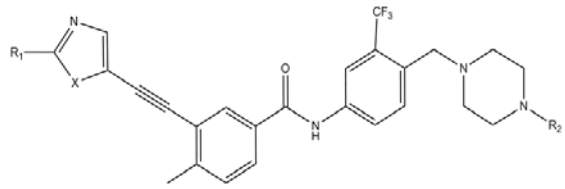

8a -8l

Compound	X	R¹	R²	Bcr-Abl	Bcr-Abl T315I
7a	CH	H	CH_3	5.3872	4.342
7b	N	H	CH_3	5.5086	4.1871
7c	CH	$NHCOCH_3$	CH_3	5.6576	5.0177
7d	CH	NHCOCH2CH3		5.6021	4.8729
***7e**	CH	$CONH_2$	CH_3	5.585	4.7447
7f	N	NHC_3	CH_3	3.71	3.2848
***8a**	ZH	H	CH_3	3.1367	2.2412
***8b**	NCH_3	H	CH_3	4.3665	3.1494
8c	NCH_3	CH_3	CH_3	5.0706	4.1612
8d	NCH_3	$CONH_2$	CH_3	5.8861	5.1192
8e	NCH_3	$CONHCH_3$	CH_3	5.7696	5.3979
8f	NCH_3	$CONHCH_2CH_2OH$	CH_3	5.4089	4.1938
8g	NCH_3	$CONH_2$	CH_2CH_2OH	6.2147	5.2366
8h	NCH_3	$CONHCH_3$	CH_2CH_2OH	5.8861	5.0757
8i	NCH_3	$CONH_2$	$CH_2CH_2OCH_3$	6.1871	4.9666
8j	NCH_3	$CONH_2$	CH_2CO_2H	5.1192	4.1938
8k	S	NH_2	CH_3	5.5528	4.757
***8l**	S	$NHCOCH_3$	CH_3	6.1739	5.2596
Ponatinib			CH_3	5.9208	5.0555
***Test**					

Table 1: The chemical structure of the inhibitor and the biological activity of pIC50.

regression models (MLR), support vector machine models (SVM), and Bayesian networks models (BN). After that, we used test set compounds to test these models for model accuracy assessment.

Multivariate linear regression is a linear approach modeling two or more variables by linear fitting to construct a function that explains the relationship between variables and response variable [11]. The model equation is as follows:

$$pIC50=a_0+a_1x_1+a_2x_2+\cdots+a_nx_n$$

Where, x_i represents the *i*-th molecular property, a_i is the corresponding fitting coefficient. The MLR model was constructed with the training data set and applied for the prediction and validation. The square of the correlation coefficient (R^2) between the predicted pIC50 value and the actual pIC50 value was used to verify the accuracy of the model. Finally, the MLR model was used to predict the pIC50 of the candidate compounds in TCM library.

The most important function of SVM model is to distinguish between two types of categories of data [12]. We construct the regression support vector machine model using LibSVM [13-15]. The Gaussian radial basis function was chosen as the kernel equation:

$$K(x_i, x_k) = \exp\left[\frac{\|x_i - x_k\|^2}{2\sigma^2}\right]$$

The squared correlation coefficient (R^2) of the actual pIC50 values and predicted pIC50 values represents the accuracy of the prediction model.

A Bayesian network model is a probabilistic graphical model that represents a set of variables and their conditional dependencies via a directed network. The network can be used to compute the probabilities of the presence of various data categories. We discretize the training data and the test data into data binning according to the pIC50 values. Linear regression analysis was then performed for each pIC50 binning. The Bayesian Network Toolbox (BNT) [16] of Matlab was used to construct the Bayesian Network model for predicting the pIC50 binning of the training data. Assuming that then *i*-th pIC50 binning has *n* compounds, let y_{ij} and x_{ijp} represent the pIC50 value of *j*-th compound in the training data and the *p*-th molecular property.

Therefore, the regression model of data set $\{y_{ij}, x_{ij1} \ldots x_{ijp}\}_{j=1}^{n}$ can represent as follows:

$$y_i = x_i \beta_i + \varepsilon_i$$

$$y_i = \begin{bmatrix} y_{i1} \\ y_{i2} \\ \vdots \\ y_{in} \end{bmatrix}, x_i = \begin{bmatrix} x_{i11} \cdots & x_{i1p} \\ x_{i21} \cdots & x_{i2p} \\ \vdots \quad \vdots & \vdots \\ x_{in1} \cdots & x_{inp} \end{bmatrix}$$

Where β_i and ε_i are the regression coefficients and error terms for the *i*-th pIC50 binning. The unknown regression coefficients β_i can use the least square method to estimate.

$$\hat{\beta}_i = \left(x_i^T x_i\right)^{-1} x_i^T y_i$$

Then the pIC50 value of the *k*-th binning can be predicted by the following equation:

$$\mathrm{plC50} = \mathrm{xk}\hat{\beta}_{\mathrm{i}}$$

The square of the correlation (R^2) between the predicted values and the actual pIC50 values can be used to verify the accuracy of the model.

As described above, the screen flowchart of the candidate compounds is shown in Figure 1.

Results and Discussion

Molecular docking

The docking simulation was based on the binding interaction with the TCM chemicals. The referent compound was Ponatinib. We also implemented the molecular docking for first and second generation drugs. After assessing the DockScore and the ADMET pharmacokinetic properties of candidate compounds, we propose four potential inhibition compounds (Figure 2). There are salvianolic acid, baicalin, 1,4-dicaffeoylquinic acid, and dihydroisotanshinone I.

The docking score is shown in Table 2. It was found that Salvianolic acid C, Baicalin, and 1,4-Dicaffeoylquinic acid had high docking values with Bcr-Abl fusion protein and Bcr-Abl T315I protein, respectively. The Dock Score of the previous three candidate compounds were higher than first and second generation drugs and Ponatinib.

The pharmacokinetic properties of Ponatinib, first and second generation drugs, and the TCM candidate compounds are shown in

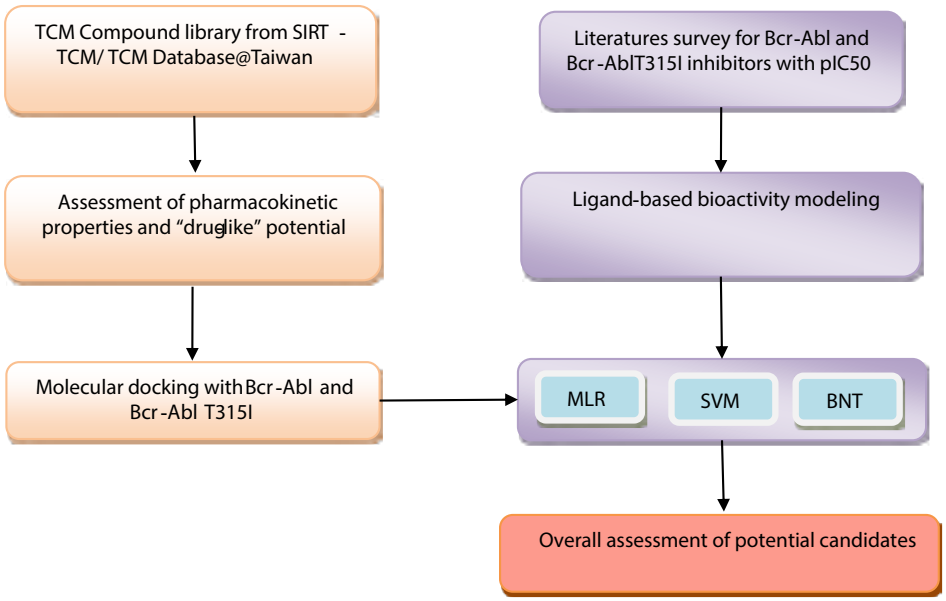

Figure 1: The screen flowchart of the candidate compounds.

Compound Name	Dock Score	
	Bcr-Abl	Bcr-AblT315I
Salvianolic acid C	108.638	139.305
Baicalin	49.773	89.272
1,4-Dicaffeoylquinic acid	48.086	94.67
Dihydroisotanshinone I	10.603	38.827
Imatinib	14.866	48.724
Nilotinib	10.699	69.571
Dasatinib	5.314	47.047
Bosutinib	-	37.654
***Ponatinib**	-	62.904
***Control**		

Table 2: Ponatinib, Imatinib, Nilotinib, Dasatinib, Bosutinib and top TCM compounds docking score.

Table 3. The properties regarding absorption, solubility, hepatotoxicity, and plasma protein binding were evaluated.

The binding interaction for the candidate compounds is shown in Figures 3.1 and 3.2. Nilotinib binds to Arg332 of Bcr-Abl with a single hydrogen bond (Figure 3.1A). Imatinib binds to Phe 439 of Bcr-Abl with a single hydrogen bond (Figure 3.1B). Dasatinib binds to Bcr-Abl with Leu340, Gly463, Arg332, Tyr435, and Ala337 via double hydrogen bonds, π-cation, and π-σ bonds (Figure 3.1C). 1,4-Dicaffeoylquinic acid through their three hydrogen bonds H55-O12, H56-O28, and H63-O8 bonding Bcr-Abl (Figure 3.1D). Baicalin binds Tyr435 of Bcr-Abl by a double hydrogen bond (Figure 3.1E). Salvianolic acid C binds to Gly463, Ala337, and Ala433 on Bcr-Abl with three hydrogen bonds (Figure 3.1F). Dihydroisotanshinone I bind to Pro465 of Bcr-Abl with a π-σ bond (Figure 3.1G).

Ponatinib binds to Phe91 and Leu144 on Bcr-Abl T315I by π-σ and π-σ bonds (Figure 3.1H). Nilotinib binds to Asn142 and Lys45 on Bcr-AblT315I with a single hydrogen bond and a π-cation (Figure 3.2I). Imatinib binds to Lys45, Asp155, and Arg141 on Bcr-AblT315I with three hydrogen bonds (Figure 3.2J). Dasatinib binds to Asn96, Asn142, and Val30 on Bcr-AblT315I with double hydrogen bonds and π-σ bonds (Figure 3.2K). Bosutinib binds to Arg141 and Lys45 on Bcr-Abl T315I with a single hydrogen bond and a π-cation (Figure 3.2L). 1,4-Dicaffeoylquinic acid binds to Gly24, Asn142, Asp155, Leu22, and Arg141, which are bonded to Bcr-AblT315I by four hydrogen bonds and π-cations (Figure 3.2M). Baicalin binds to Lys45, Asp155, Asn142, and Arg141 on Bcr-AblT315I with four hydrogen bonds (Figure 3.2N). Salvianolic acid C binds to Lys45, Glu60, and Lys45 on Bcr-AblT315I (Figure 3.2O) with a double hydrogen bond and a π-cation. Dihydroisotanshinone I bind to Leu144 of Bcr-AblT315I with a π-σ bond (Figure 3.2P).

Hydrophobic interaction analysis by LigPlot [17] is shown in Figure 4. Salvianolic acid C interact with Bcr-Abl (Figure 4F) were more stable than the first and second generation drugs of Imatinib, Nilotinib and Dasatinib (Figure 4A-4C). The TCM candidate compounds 1,4-Dicaffeoylquinic acid (Figure 4N), Baicalin (Figure 4M), and Salvianolic acid C (Figure 4O) interact with Bcr-AblT315I are more stable than Ponatinib (Figure 4H), Imatinib, Nilotinib, Bosutinib, and Dasatinib (Figure 4I-4L).

Quantitative Structure-Activity Relationship (QSAR) model for predicting biological activity

We used a set of known tyrosine kinase inhibitors to construct QSAR models based on their molecular descriptors. The molecular descriptors of 204 biological properties were analyzed by GFA, and the best 8 molecular descriptors were selected to construct MLR model, SVM model, and BNT model. In the model of Bcr-Abl, these molecular characterizations include a description of the molecular properties of ES_Sum_aaN, Kappa_2, Jurs_PNSA_1, Jurs_PNSA_3, and Shadow_XY. In the Bcr-AblT315I model, these molecular characterizations include descriptions of the molecular properties of ES_Sum_ssNH, Num_RotatableBonds, Jurs_FPSA_1, Shadow_XY, and Molecuar_Volume. Molecular characteristics symbol and description are shown in Table 4 [18].

Based on these molecular properties we obtain the MLR model equation as follows,

Bcr-Abl in the MLR model equation:

GFATempModel_1=-9.5632+0.25115 × ES_Sum_aaN-0.72782 ×

	Pharmacokinetic properties			
	Absorption[1]	**Solubility[2]**	**Hepatotoxicity[3]**	**PPB[4]**
Salvianolic acid C	3	2	1	1
Baicalin	3	3	1	0
1,4-Dicaffeoylquinic acid	3	3	1	0
Dihydroisotanshinone I	0	2	1	2
Imatinib	0	2	1	1
Nilotinib	1	1	1	2
Dasatinib	0	2	0	2
Bosutinib	0	2	1	1
***Ponatinib**	0	1	0	2
***Control**				
[1]Absorption (Human intestinal absorption): 0 (good absorption), 1 (moderate absorption), 2 (poor absorption), 3 (very poor absorption).				
[2]Solubility: 0 (extremely low), 1 (very low, but possible), 2 (low), 3 (good), 4 (optimal), 5 (too soluble), 6 (warning).				
[3]Hepatotoxicity: 0 (nontoxic), 1 (toxic).				
[4]PPB (Plasma protein binding): 0 (binding is <90%), 1 (binding is >90%), 2 (binding >95%).				

Table 3: Predicted pharmacokinetic properties of Ponatinib, Imatinib, Nilotinib, Dasatinib, Bosutinib, and TCM candidates.

Symbol	Description
ES_Sum_aaN	The sum of the electrotopological state value for atom type aaN, "a" represents an aromatic bond and "N" is the nitrogen atom.
Kappa_2	Kier's Second Order Shape Index.
Jurs_PNSA_1	Partial Negative Surface Area.
Jurs_PNSA_3	Atomic Charge Weighted Negative Surface Area.
Shadow_XY	Shadow Index for the XY lane.
ES_Sum_ssNH	The sum of the electrotopological state value for atom type ssNH, "s" is the single bond and NH group.
Num_RotatableBonds	The numbers of bonds which allow free rotation around themselves.
Jurs_FPSA_1	Fractional Charged Partial Surface Area: PPSA-1/MW.

Table 4: Molecular properties symbol description.

	Predicted bioactivity (pIC50)							
	Bcr-Abl				Bcr-Abl T315I			
	MLR	SVM	Bayesian		MLR	SVM	Bayesian	
Salvianolic acid C	2.8039	6.4417	5.1830		3.1128	4.3296	2.7189	
Baicalin	0.2134	6.2736	4.2024		4.9290	4.8770	2.4946	
1,4-Dicaffeoylquinic acid	2.0146	6.4612	5.3877		4.8347	4.8678	3.0767	
Dihydroisotanshinone I	0.0703	5.3503	2.5746		1.1831	3.1293	1.7627	
Imatinib	2.9274	4.4650	3.0808		2.3600	3.7270	3.0539	
Nilotinib	9.1560	5.6713	4.5432		3.9338	4.7390	2.9824	
Dasatinib	3.8592	4.9367	3.4534		1.0876	3.2628	2.8913	
Bosutinib	3.5488	5.1557	3.9247		3.3402	4.0499	3.2361	
***Ponatinib**	5.8950	5.3642	5.8820		5.0555	4.7448	5.1949	
***Control**								

Table 5: Predicted bioactivity predictions (pIC50) of Ponatinib, Imatinib, Nilotinib, Dasatinib, Bosutinib and TCM candidates using MLR, SVM, and Bayesian Network models.

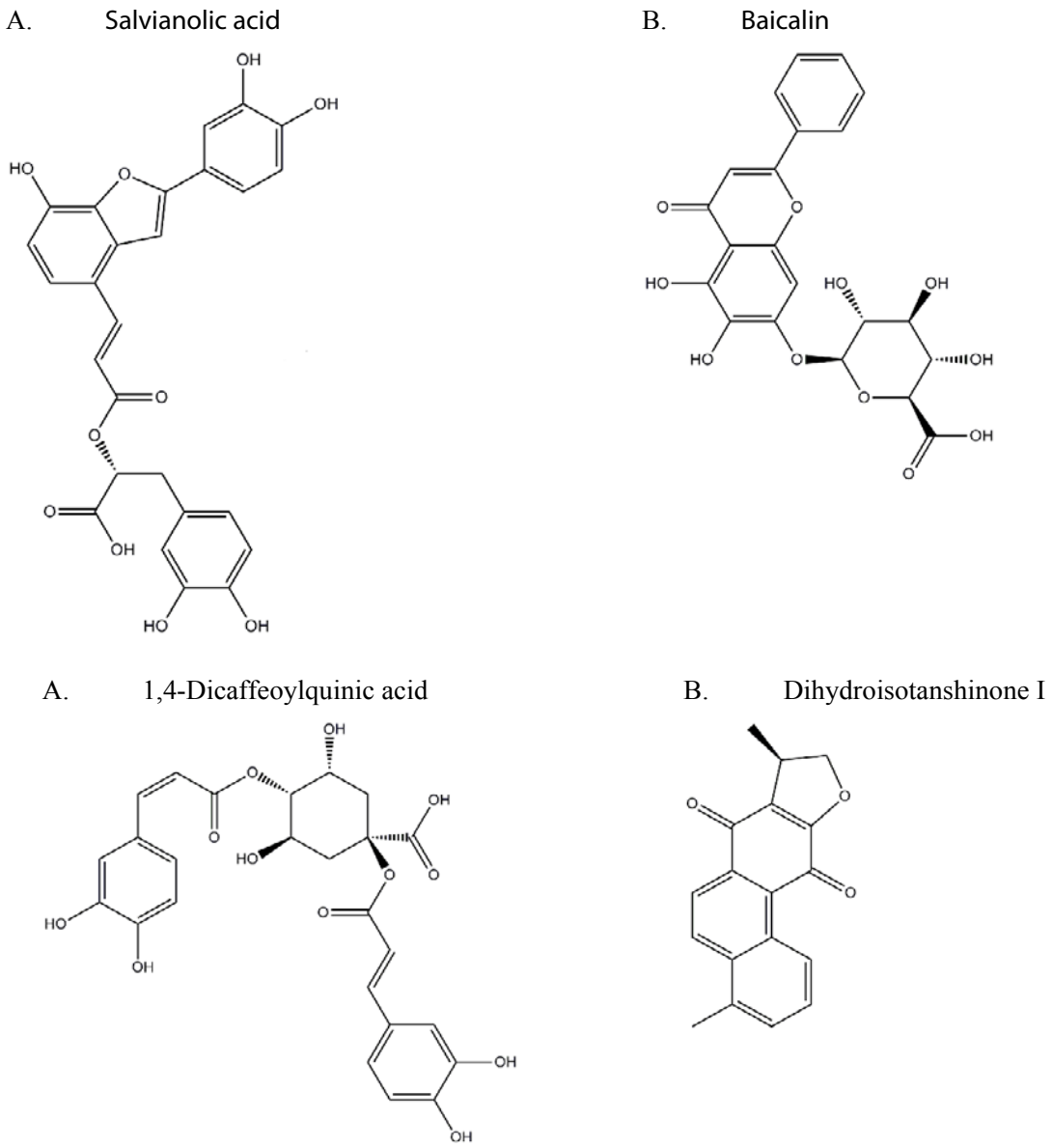

Figure 2: The chemical structure of Chinese herbal components for treating CML candidate compounds.

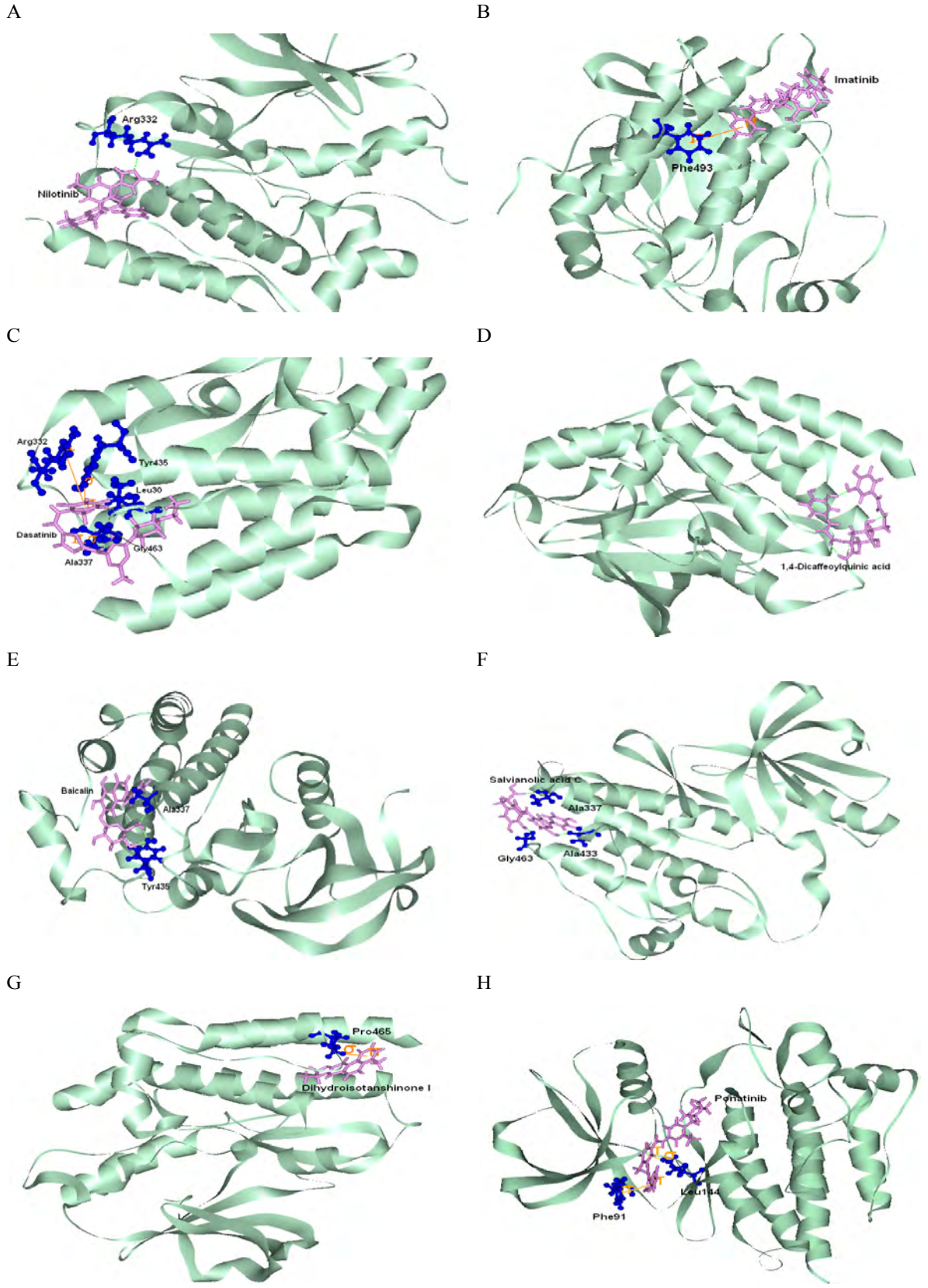

Figure 3.1: Docking pose on Bcr-Abl regarding A (Nilotinib), B (Imatinib), C (Dasatinib), D (1,4-Dicaffeoylquinic acid), E (Baicalin), F (Salvianolic acid C), G (Dihydroisotanshinone I). H (Ponatinib docking with Bcr-AblT315I).

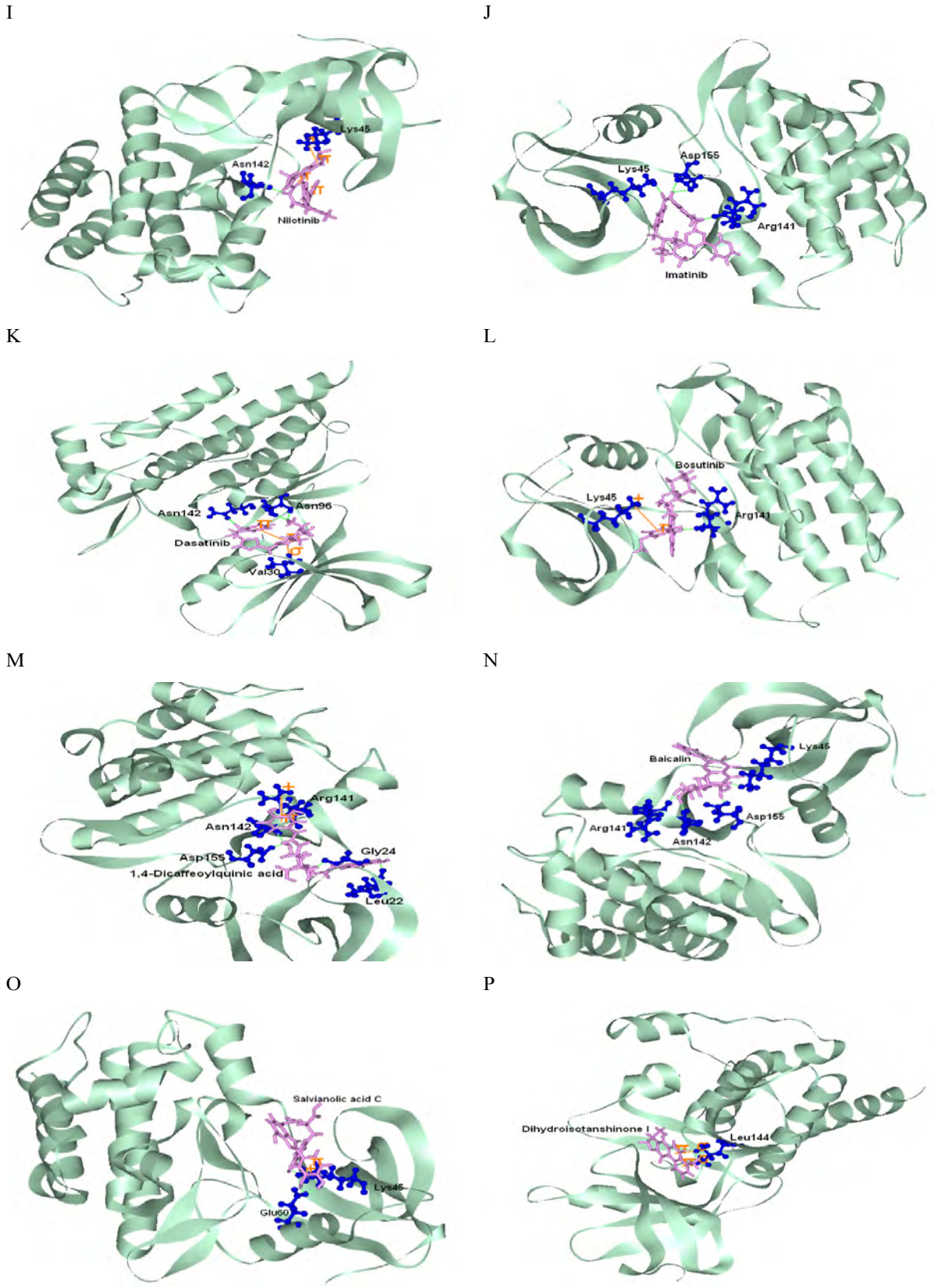

Figure 3.2: Docking pose on Bcr-Abl T315I regarding I (Nilotinib), J (Imatinib), K (Dasatinib), L (Bosutinib), M (1,4-Dicaffeoylquinic acid), N (Baicalin), O (Salvianolic acid C), P (Dihydroisotanshinone I). Inhibitors are stick. Blue, green, and orange contours denote amino acid, hydrogen bonds, and pi-bonds, respectively.

Citation: Xiao Y, Chang PC, Tsai JJP (2018) The Potential Inhibitors in Traditional Chinese Medicine for BCR-ABL T315I Mutation of Chronic Myelogenous Leukemia. Med Chem (Los Angeles) 8: 066-078. doi: 10.4172/2161-0444.1000496

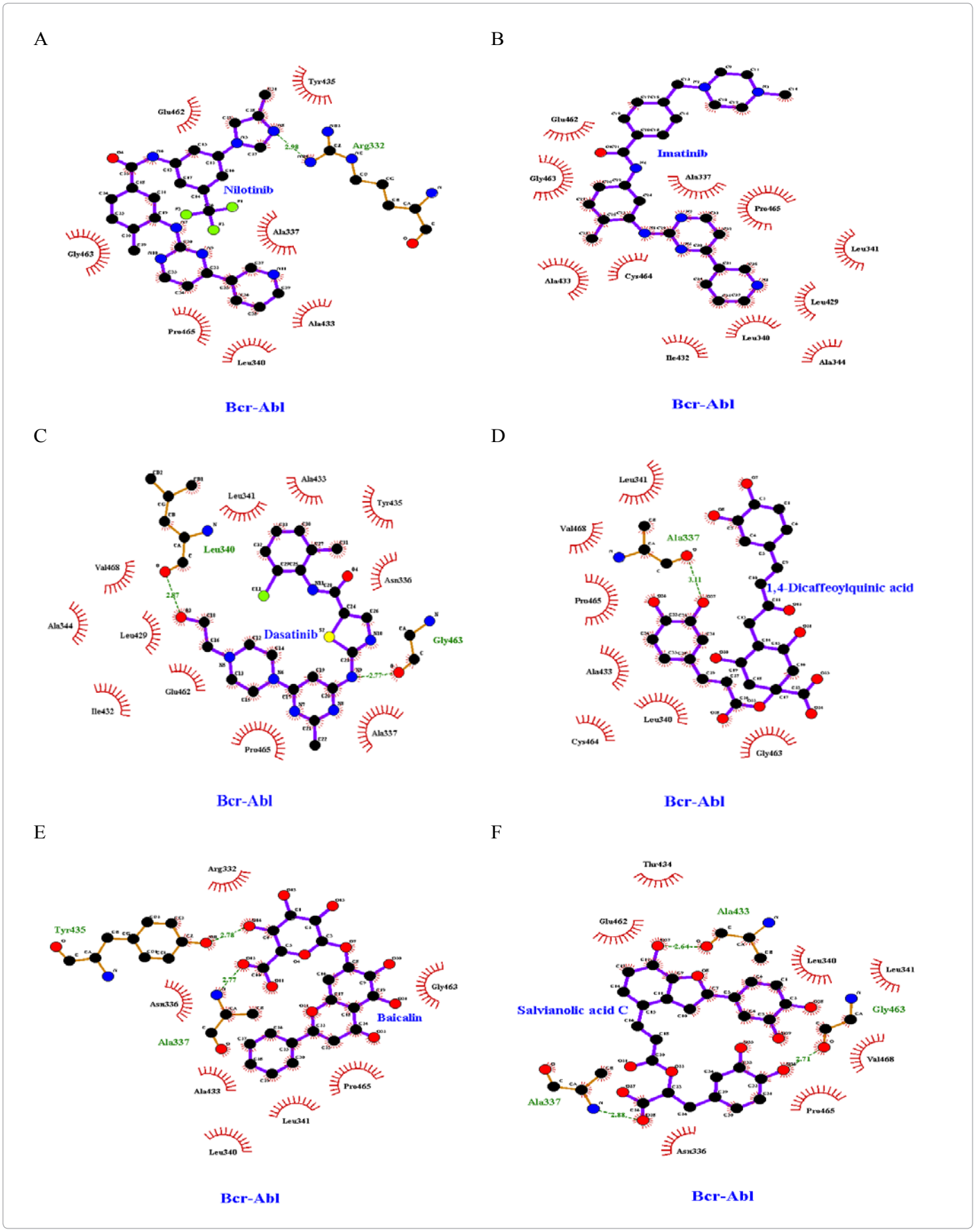

G

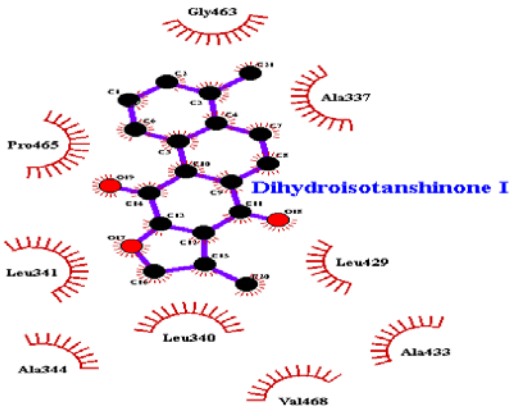

Bcr-Abl

H

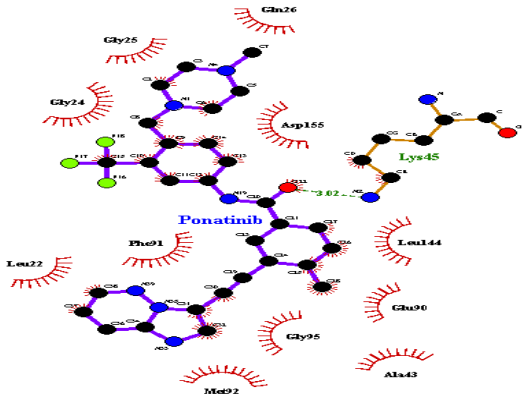

Bcr-AblT315I

I

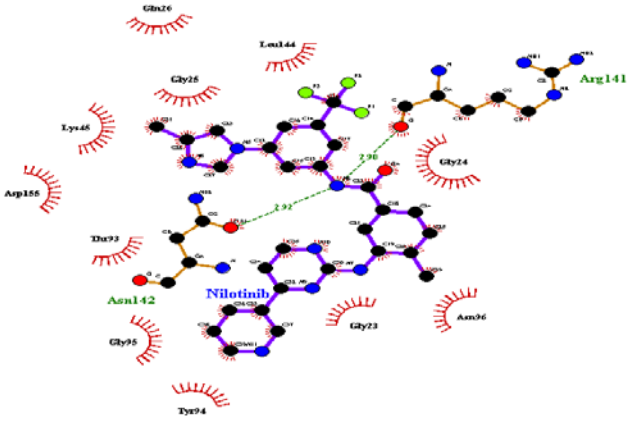

Bcr-AblT315I

J

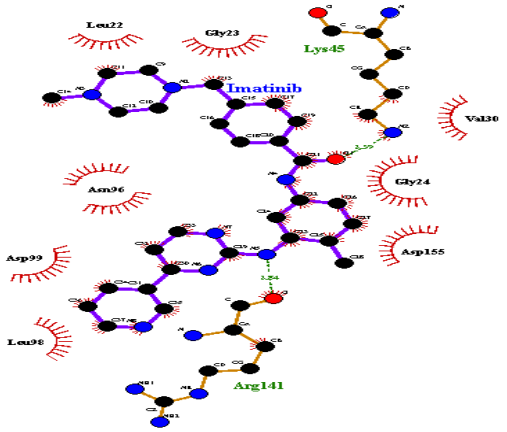

Bcr-AblT315I

K

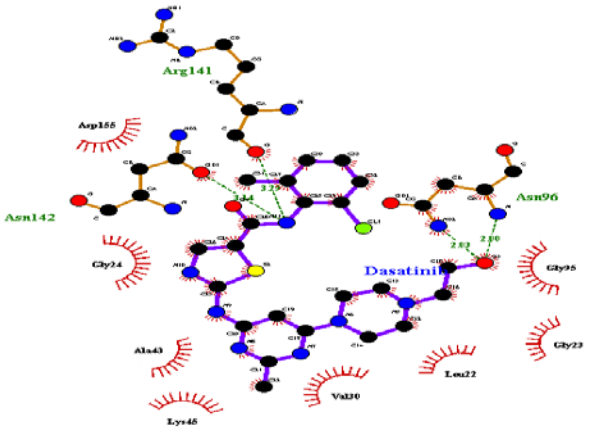

Bcr-AblT315I

L

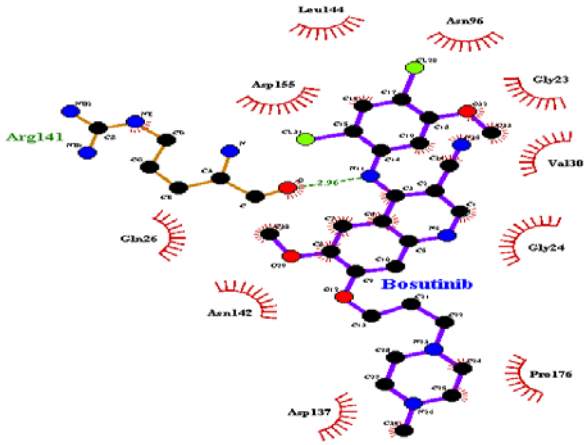

Bcr-AblT315I

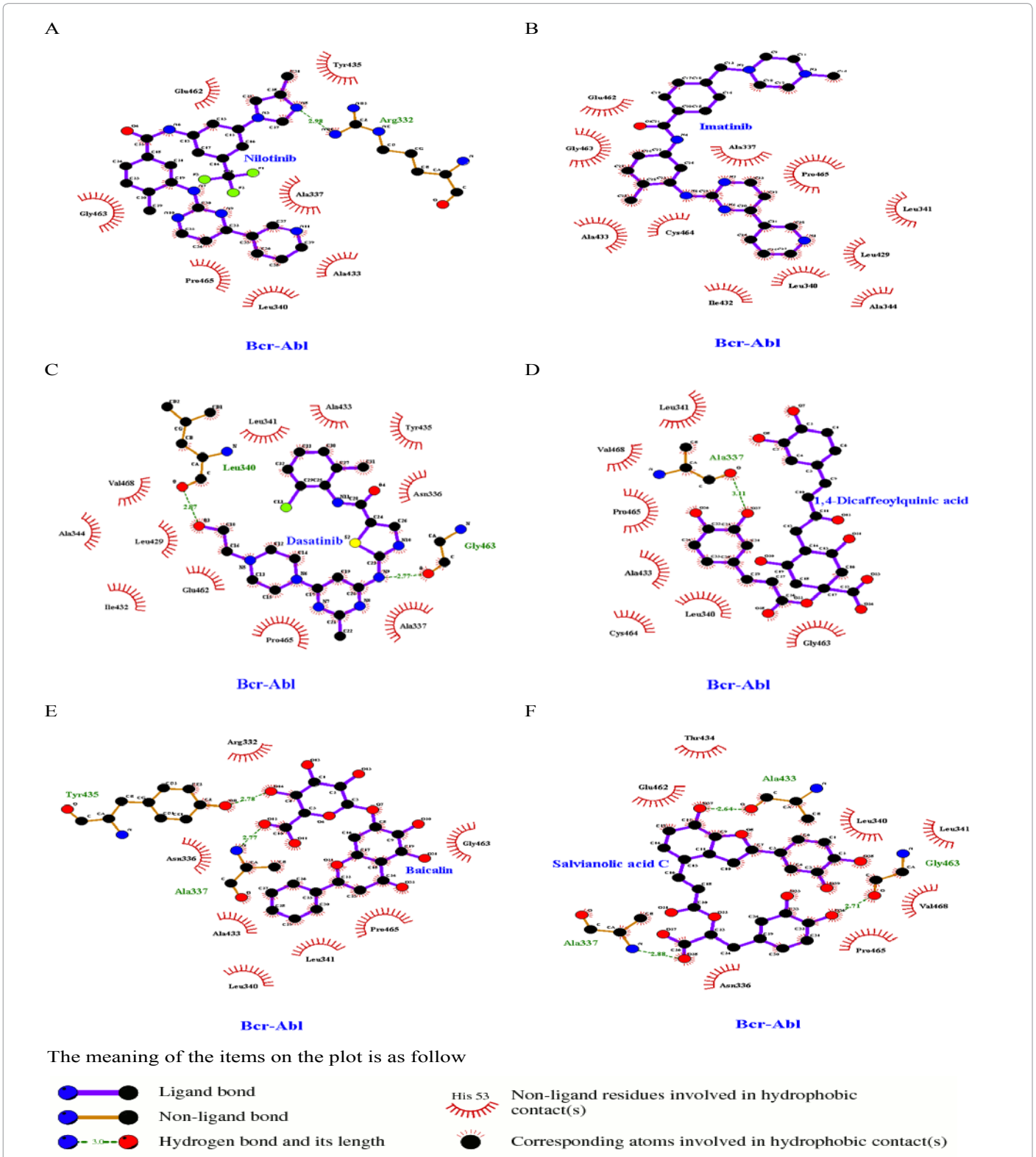

Figure 4: Analysis of hydrophobic interactions during docking by LigPlot. Docking pose with Bcr-Abl for A (Nilotinib), B (Imatinib), C (Dasatinib), D (1,4-Dicaffeoylquinic acid), E (Baicalin), F (Salvianolic acid C), and G (Dihydroisotanshinone I). Docking poses with Bcr-AblT315I for H (Ponatinib docking with Bcr-AblT315I), I (Nilotinib), J (Imatinib), K (Dasatinib), L (Bosutinib), M (1,4-Dicaffeoylquinic acid), N (Baicalin), O (Salvianolic acid C), P (Dihydroisotanshinone I). Bonds: ligand bonds, non-ligand bonds, hydrogen bonds, and hydrophobic is purple, orange, olive green, and brick red, respectively. Atoms: nitrogen, oxygen, carbon, and sulphur are blue, red, black, and yellow, respectively. Labels: plot title, ligand residue name, non-ligand residue name, hydrophobic residue name, ligand atom name, and non-ligand atom name are blue, blue, olive green, blue, black, and black, respectively. Black, red, yellow, blue, and green denote carbon, oxygen, sulfur, nitrogen, and fluorine, respectively.

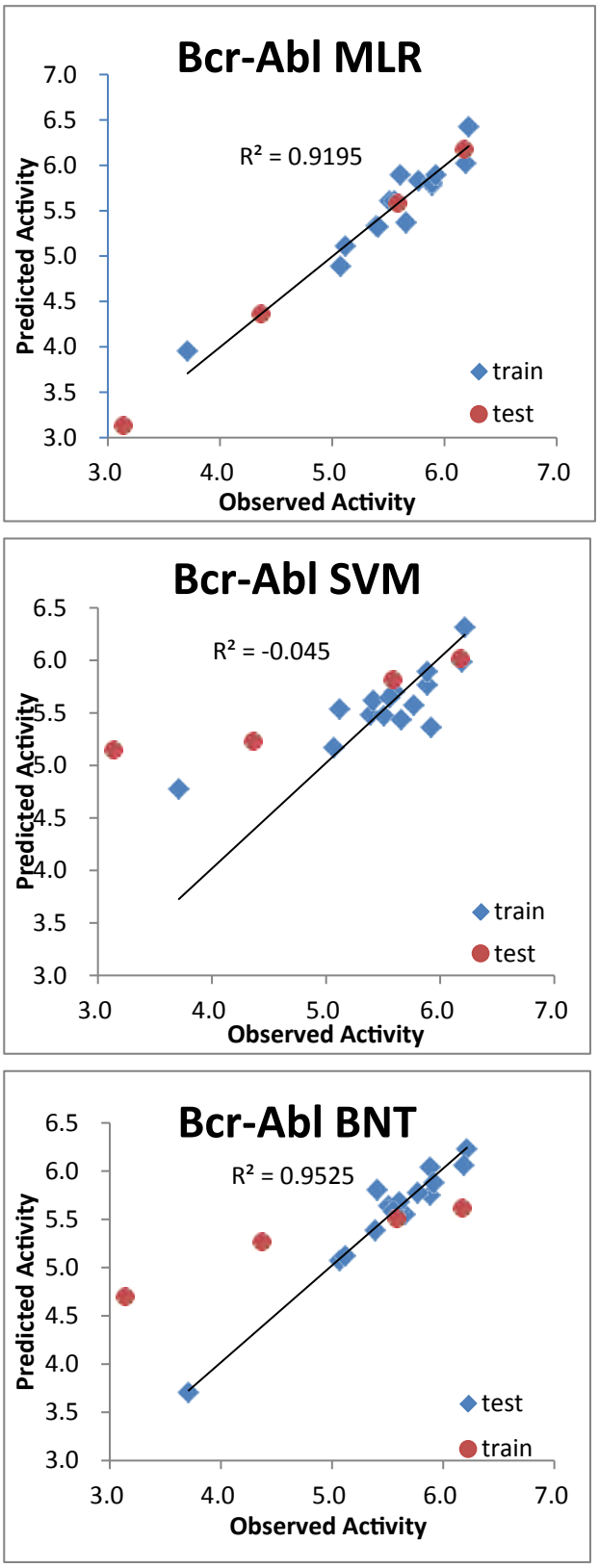

Figure 5: Correlation of observed and predicted activity (pIC50) using 2D-QSAR models of Bcr-Abl with MLR, Bayesian Network model, and SVM models.

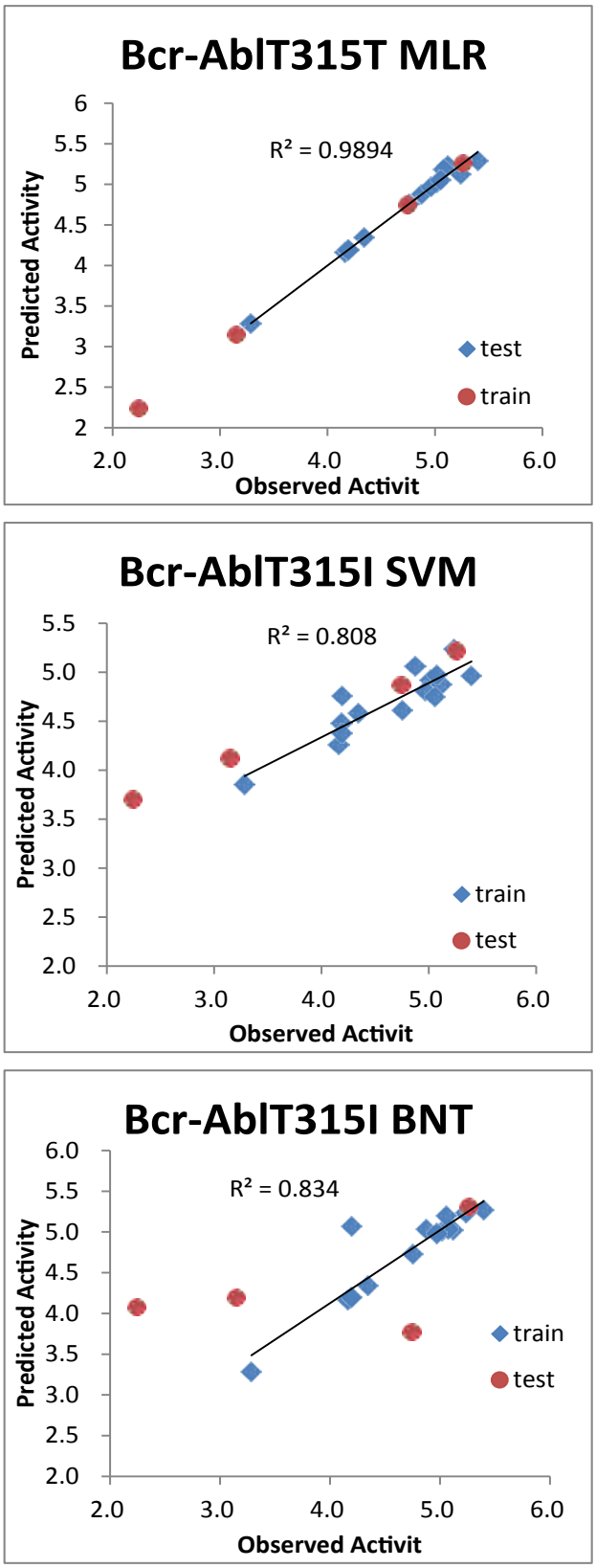

Figure 6: Correlation of observed and predicted activity (pIC50) using 2D-QSAR models of Bcr-AbT315II with MLR, Bayesian Network model, and SVM models.

Kappa_2+0.06373

× Jurs_PNSA_1+0.12023×Jurs_PNSA_3+0.071349 × Shadow_XY

Bcr-AblT315I in the MLR model equation:

GFATempModel_2=-5.8619-0.31832 × ES_Sum_ssNH-1.1364 × Num_RotatableBonds-15.867 × Jurs_FPSA_1+0.050214 × Shadow_XY+0.070524 × Molecuar_Volume

The correlation between the pIC50 observations of Bcr-Abl and the predictions from the 2D-QSAR model is shown in Figure 5. The correlation between the pIC50 observations of Bcr-AblT315I and the predicted values using the 2D-QSAR model is shown in Figure 6. The correlation coefficient R^2 value of Bcr-Abl in the 2D-QSAR MLR model is 0.913. The correlation coefficient R^2 of the SVM model is 0.712. The BNT model correlation coefficient R^2 is 0.952 (Figure 5). Besides the SVM model (R^2=0.712) is less than 0.8, the remaining models all are >0.8, with a high correlation. On the other hand, the R^2 value of the BCR-Abl T315I in the 2D-QSAR model is 0.989, the R^2 value of the SVM model is 0.808, and the R^2 value of the BNT model is 0.834 (Figure 6). All models are >0.8, with a high degree of correlation.

We used the 2D-QSAR model of MLR, SVM model, and BNT model to predict the biological activity (pIC50) of currently approved drugs of CML treatment and TCM candidate compound. The results are shown in Table 5.

Salvianolic acid C is present in Danshen. Baicalin was found in Bing Tou Huang Qin, Chuan Huang Qin, Da Che Qian, Baihua Dan Shen, Dian Huang Qin, Gan Su Huang Qin, Mu Hudie, Mu Hu Die Shu Pi, and Zhan Mao Huang Qin. It mainly found in the Huang Qin. 1,4-Dicaffeoylquinic acid is present in Cang Er, and Dihydroisotanshinone I can be extracted from Bai Huad Dan Shen. Danshen is widely used in Chinese herbal medicine to promote circulation to improve the effectiveness of blood flow, often used in the treatment of many diseases, including cancer [19,20]. The main components Danshen are hydrophilic phenolic acids and lipophilic tanshinones with anti-cancer effect [21,22]. Salvianolic acid C is a phenolic compound in Danshen. Baicalin is a component of Huang Qin. Previous studies show that baicalin has therapeutic effects on cancer [23-27]. Cang Er in Chinese medicine used in the treatment of typhoid fever caused by headache, sinusitis, urticarial, and arthritis [28]. The composition caffeoylquinic acids have the efficacies of antioxidant activity, anti-inflammatory, anti-microbial effects, enzyme inhibition, inhibition of platelet aggregation [29]. DihydroisotanshinoneI is one of the components of Danshen, against various cancer cell cytotoxicity [30,31], which can inhibit the proliferation of the endothelial cells and anti-angiogenesis and induce cell growth arrest in S phase to cause apoptosis.

Conclusion

We performed structure-based virtual screening and QSAR modeling to select potential TCM candidate compounds. The results show that salvianolic acid C, baicalin, 1,4-dicaffeoylquinic acid, and dihydroisotanshinone I might have the potential to treat Chronic Myelogenous Leukemia with fewer side effects.

Acknowledgments

The research was supported by grants from the Ministry of Science and Technology of Taiwan (MOST 104-2221-E-468-015, MOST 105-2632-E-468-002) and Asia University (105-asia-14).

References

1. Dameshek W (1951) Editorial: Some Speculations on the Myeloproliferative Syndromes. Blood 6: 372-375.
2. McGee MM, Campiani G, Ramunno A, Fattorusso C, Nacci V, et al. (2001) Pyrrolo-1,5-benzoxazepines induce apoptosis in chronic myelogenous leukemia (CML) cells by bypassing the apoptotic suppressor bcr-abl. J Pharmacol Exp Ther 296: 31-40.
3. Santos FP, Kantarjian H, Quintás-Cardama A, Cortes J (2011) Evolution of therapies for chronic myelogenous leukemia. Cancer J 17: 465-476.
4. Lamontanara AJ, Gencer EB, Kuzyk O, Hantschel O (2013) Mechanisms of resistance to BCR-ABL and other kinase inhibitors. Biochimica et Biophysica Acta 1834: 1449-1459.
5. Thomas M, Huang WS, Wen D, Zhu X, Wang Y, et al. (2011) Discovery of 5-(arenethynyl) hetero-monocyclic derivatives as potent inhibitors of BCR-ABL including the T315I gatekeeper mutant. Bioorganic and Medicinal Chemistry Letters 21: 3743-3748.
6. Naviglio S, Caraglia M, Abbruzzese A, Chiosi E, Di Gesto D, et al. (2009) Protein kinase A as a biological target in cancer therapy. Expert Opin Ther Targets 13: 83-92.
7. Levinson NM, Kuchment O, Shen K, Young MA, Koldobskiy M, et al. (2006) A Src-Like Inactive Conformation in the Abl Tyrosine Kinase Domain. PLoS Biology 4: e144.
8. Modugno M, Casale E, Soncini C, Rosettani P, Colombo R, et al. (2007) Crystal Structure of the T315I Abl Mutant in Complex with the Aurora Kinases Inhibitor PHA-739358. Cancer Research 67: 7987-7990.
9. SIRCoTCM (2016) Shanghai Innovative Research Center of Traditional Chinese Medicine (SIRC/TCM). Available from: http://www.sirc-tcm.sh.cn/en/index.html Accessed on: April 05, 2018.
10. Chen CY (2011) TCM Database@Taiwan: The World's Largest Traditional Chinese Medicine Database for Drug Screening In Silico. PLoS ONE 6: e15939.
11. Slinker BK, Glantz SA (2008) Multiple Linear Regression: Accounting for Multiple Simultaneous Determinants of a Continuous Dependent Variable. Circulation 117: 1732-1737.
12. Alexandrov NN, Mironov AA (1963) Pattern recognition using generalized portrait method. Automation and Remote Control 24: 774-780.
13. Ivanciuc O (2007) Applications of support vector machines in chemistry. Reviews in Computational Chemistry 23: 291-400.
14. Vapnik V (1995) The Nature of Statistical Learning Theory. IEEE Transactions on Neural Networks 8: 1564.
15. Chang CC, Lin CJ (2011) LIBSVM: a Library for support vector machines. ACM Transactions on Intelligent Systems and Technology 2: 1-27.
16. Yu J, Smith VA, Wang PP, Hartemink AJ, Jarvis ED (2004) Advances to Bayesian network inference for generating causal networks from observational biological data. Bioinformatics 20: 3594-3603.
17. Wallace AC, Laskowski RA, Thornton JM (1996) LIGPLOT: a program to generate schematic diagrams of protein-ligand interactions. Protein Eng 8: 127-134.
18. Saluja AK, Tiwari M, Kumar S (2014) Ligand-based design, virtual screening, and ADME/T-based profiling on a dataset of 1,3,5-triazine-substituted benzene sulfonamides as carbonic anhydrase inhibitors. Journal of Chemometrics 28: 108-115.
19. Gong Y, Li Y, Lu Y, Li L, Abdolmaleky H (2011) Bioactive tanshinones in Salvia miltiorrhiza inhibit the growth of prostate cancer cells in vitro and in mice. Int J Cancer 129: 1042-1052.
20. Wu CF, Bohnert S, Thines E, Efferth T (2016) Cytotoxicity of Salvia miltiorrhiza Against Multidrug-Resistant Cancer Cells. Am J Chin Med 44: 871-894.
21. Chen X, Guo J, Bao J, Lu J, Wang Y (2014) The anticancer properties of Salvia miltiorrhiza Bunge (Danshen): a systematic review. Med Res Rev 34: 768-794.
22. Su CY, Ming QL, Rahman K, Han T, Qin LP (2015) Salvia miltiorrhiza: Traditional medicinal uses, chemistry, and pharmacology. Chin J Nat Med 13: 163-182.
23. Wang CZ, Zhang CF, Chen L, Anderson S, Lu F, et al. (2015) Colon cancer chemopreventive effects of baicalein, an active enteric microbiome metabolite

from baicalin. Int J Oncol 47: 1749-1758.

24. Yu Y, Pei M, Li L (2015) Baicalin induces apoptosis in hepatic cancer cells in vitro and suppresses tumor growth in vivo. Int J Clin Exp Med 8: 8958-8967.
25. Peng Y, Fu ZZ, Guo CS, Zhang YX, Di Y, et al. (2015) Effects and Mechanism of Baicalin on Apoptosis of Cervical Cancer HeLa Cells In-vitro. Iran J Pharm Res 14: 251-261.
26. Ikemoto S, Sugimura K, Yoshida N, Yasumoto R, Wada S, et al. (2000) Antitumor effects of Scutellariae radix and its components baicalein, baicalin, and wogonin on bladder cancer cell lines. Urology 55: 951-955.
27. Chen J, Li Z, Chen AY, Ye X, Luo H, et al. (2013) Inhibitory effect of baicalin and baicalein on ovarian cancer cells. Int J Mol Sci 14: 6012-6025.
28. Han T, Li HL, Hu Y, Zhang QY, Huang BK, et al. (2006) Phenolic acids in Fructus Xanthii and determination of contents of total phenolic acids in different species and populations of Xanthium in China. Zhong Xi Yi Jie He Xue Bao 4: 194-198.
29. Zhao Y, Zhao J, Li XP, Zhou CX, Sun HD, et al. (2006) Advances in caffeoylquinic acid research. Zhongguo Zhong Yao Za Zhi 31: 869-874.
30. Bian W, Chen F, Bai L, Zhang P, Qin W (2008) Dihydrotanshinone I inhibits angiogenesis both in vitro and in vivo. Acta Biochimica et Biophysica Sinica 40: 1-6.
31. Lee DS, Lee SH (2000) Biological activity of dihydrotanshinone I: effect on apoptosis. J Biosci Bioeng 89: 292-293.